

Few particle effects in the emission of short-radiative-lifetime single quantum dots

P. Senellart,* E. Peter, J. Hours, A. Cavanna, and J. Bloch

CNRS-Laboratoire de Photonique et Nanostructures, Route de Nozay, 91460 Marcoussis, France

(Received 8 February 2005; revised manuscript received 22 June 2005; published 2 September 2005)

We report on photoluminescence measurements on single GaAs monolayer fluctuation quantum dots. We show that, because the quantum dots have short radiative lifetime, the biexciton line is composed of various contributions originating from the Coulomb interaction with higher energy excitons. This appears as a broad low energy sideband on the biexciton line which appears for an average number of excitons in the system as small as 0.3. A simple model allows us to account for our observations and to show that this sideband is the spectral signature of fast quantum dots in continuous wave measurements.

DOI: [10.1103/PhysRevB.72.115302](https://doi.org/10.1103/PhysRevB.72.115302)

PACS number(s): 78.55.Cr, 78.67.Hc, 71.70.Gm, 71.35.Cc

I. INTRODUCTION

Semiconductor quantum dots (QDs) are zero-dimensional traps for electrons and holes in a three-dimensional semiconductor medium. The intensive study of their fundamental properties has led to the common image of the semiconductor “macro-atom,” and has given rise to a large interest for their use in the field of quantum cryptography and quantum computing.¹ This “macro-atom” image comes from the usual spectral properties of QDs. First, due to the zero-dimensional confinement, QDs present discrete optical transitions. Second, thanks to Coulomb interaction, the energy of the optical transitions is determined by the total number of excitons in the QD. This fundamental properties have first been evidenced by continuous wave (c.w.) photoluminescence measurements,^{2,3} and recently revisited through correlation measurements which evidence a radiative cascade in the QD emission.⁴ The understanding of the crucial role played by Coulomb interaction in the QD emission has led to theoretical proposals to use QDs for quantum bit generation^{1,5} and to first experimental demonstrations of quantum functionalities. For instance, all optical quantum gates^{6,7} and single photon sources^{8,9} based on QDs have recently been demonstrated. For such applications and other like indistinguishable photon sources, short radiative lifetime QDs are needed. To find out the best system, various QDs are investigated, such as II-VI QDs with a radiative lifetime of $\tau=300$ ps,¹¹ InGaAs QDs ($\tau=400$ ps),¹⁰ Recently, we have evidenced that the radiative lifetime of a GaAs QD can be as short as 100 ps for the exciton (X) and 60 ps for the biexciton (XX) and is controlled by its lateral size.¹² In the present work, we show that, whenever one deals with fast QDs, few particule effects have to be revisited to describe the QD emission.

We report on photoluminescence measurements on QDs formed at the interface fluctuation of a thin GaAs quantum well under continuous wave nonresonant excitation. When increasing the excitation power, a low energy sideband to the biexciton line develops. The sideband appears for an average number of excitons in the system as small as 0.3. We show that this sideband is the result of the biexciton coulombian interaction with the continuum of higher energy excitons. We develop a rate equation model describing the emission of these QDs under c.w. excitation, which perfectly accounts

for our experimental observations. It shows that the appearance of the biexciton sideband at very low number of excitons in the system is the result of the very fast radiative lifetime of GaAs quantum dots. Finally, to further analyze the influence of the radiative lifetime on the biexciton sideband, we extend our model to compare the case of fast QDs to slow QDs.

II. EXPERIMENTAL OBSERVATIONS

The sample under study consists of a nominally 10 monolayer GaAs quantum well embedded in $\text{Al}_{0.33}\text{Ga}_{0.67}\text{As}$ barriers. The description of the sample growth and its optical characterization are detailed in Ref. 9. To isolate single QDs, microdisk structures have been chemically etched. Measurements are performed at a sample temperature of 8 K using a cold-finger helium cryostat. Micro-photoluminescence (μ -PL) measurements are performed in the far field using a microscope objective, with an excitation spot diameter of $2\ \mu\text{m}$. The excitation beam is delivered by a continuous wave (c.w.) Ti:sapphire laser with energy around 1.73 eV. The signal is detected by a N_2 -cooled Si CCD camera with a 0.1 meV spectral resolution.

The insert of Fig. 1(a) shows a c.w. photoluminescence (PL) spectrum on a large energy scale for an excitation power of $P=1.35\ \mu\text{W}$. On the high energy side, the broad emission corresponds to the radiative recombination of excitons in the QW. On the low energy side, two discrete lines labelled X and XX appear, attributed to the emission of a single QD named QD1, as explained below. Figure 1(a) presents the emission of QD1, for various excitation powers. The spectra have been normalized to the peak intensity of the exciton line, at the energy of 1.6988 eV. At the energy of 1.6962 eV, a second line appears when increasing the excitation power. On the low energy side of this line, a broad emission develops when increasing the excitation power. To identify the origin of these lines, we consider the spectrally integrated intensity of the emission line as a function of the excitation power. For low excitation density, the exciton line increases linearly with excitation power. Meanwhile, the integrated intensity of the low energy line, as well as its sideband, increases quadratically. These observations indicate that the emission originates from the recombination of exci-

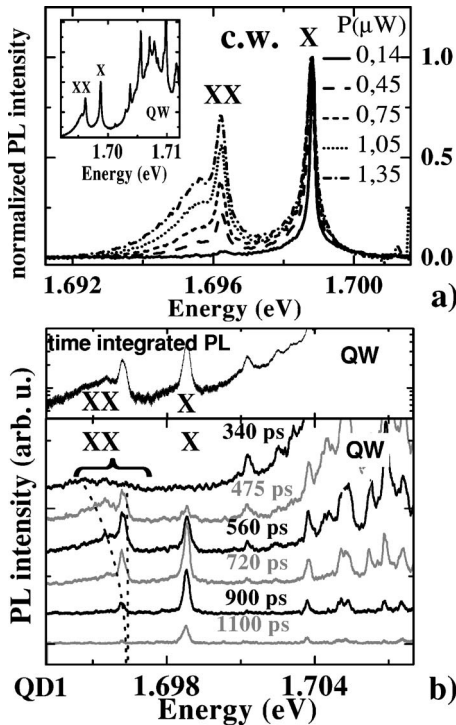


FIG. 1. (a) PL spectra of QD1 for various excitation powers P under c.w. excitation. The spectra are normalized to the X peak intensity. Insert: broad energy spectrum for $P=1.35 \mu\text{W}$. (b) Photoluminescence spectra under nonresonant pulsed (3 ps) excitation. Top: time integrated spectrum. Bottom: spectra for different time delays after the excitation pulse.

ton (X) and biexciton (XX) inside the QD. This analysis is confirmed by time resolved measurements.¹² Figure 1(b) shows the emission spectra obtained on the same QD under nonresonant pulsed (ps) excitation for various time delay after the excitation pulse. First, the biexciton line, including its sideband, is emitted before the exciton line. Moreover, as the QW excitons radiatively recombine, the emission of the QD biexciton first takes place in the low energy part of the sideband, then in its high energy part, and finally at the bare XX energy. These observations allow us to rule out the presence of charged excitons in the system which would radiate simultaneously to the exciton.¹³ Lastly, note that the sideband to the XX line remains unchanged if we change the excitation energy. QD charging is known to depend strongly on the excitation energy,¹⁴ a dependence we do not observe here. As a result, we can conclude that the sideband observed on the low energy side of the biexciton line is the result of various multiexciton lines corresponding to the radiative recombination of a biexciton in the QD while higher energy excitons are in weakly localized states of the 2D quantum well. In the following, we refer to the gathering of these multiexcitonic lines as to the “XX sideband.”

We observe this low energy sideband on the biexciton line on every single QD we have studied, from several samples presenting monolayer fluctuation QDs. The sideband appears whenever the biexciton emission is observed. However, the contribution of the sideband to the biexciton emission varies from dot to dot. To qualitatively understand the appearance

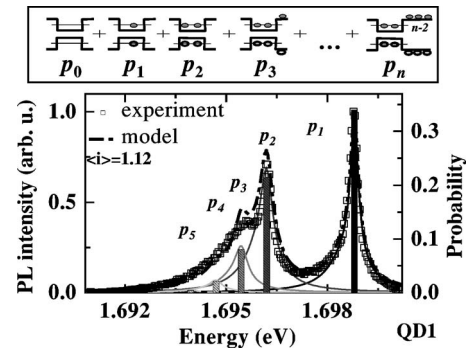


FIG. 2. Top: representation of the various occupations i of the system contributing to the c.w. PL signal with probability p_i . Bottom: Squares: experimental spectrum of QD1 for $\langle i \rangle = 1.12$ corresponding to an excitation power of $1.35 \mu\text{W}$. Bars: probabilities p_i . Full lines: spectral function with unity area multiplied by p_i . Dotted-dashed line: calculated spectrum.

of this sideband, let us analyze the origin of the discrete lines in the PL signal under continuous wave excitation. To simplify, we consider that the QD only contains one confined state. This assumption well applies for the QDs under study since we measured no excited states by photoluminescence excitation spectroscopy as in Ref. 15. We consider the system composed of the QD and its immediate surrounding, i.e., the QW states from which excitons can scatter toward the QD. These states can be pure 2D states or weakly localized states. We define i as the number of excitons in the system. The c.w. PL signal is the sum of the radiative signal emitted by the system for each number of excitons i for i varying from $i=0$ to $i=\infty$ with a weight q_i . q_i will be explicitly calculated later in the paper. Each case corresponding to each value of i is illustrated in the upper part of Fig. 2. The system occupation $i=1$ gives rise to an emission at the energy of the exciton $E_1=E_X$; when $i=2$, the emission occurs at the unperturbed biexciton energy $E_2=E_{XX}$.

For $i \geq 3$, the system radiates either through the QW or through the QD. In this case, the QD emission takes place at an energy that is redshifted as compared to the biexciton energy, as we explain below. In the following, we show that the QD emission spectral shape is governed by the relative X and XX lifetime with respect to the QW lifetime. Time resolved measurements have shown that QD1 presents an X (resp. XX) radiative lifetime of 150 ps (resp. 100 ps). The QW radiative lifetime has been measured to be 160 ps. In the following, we show that when the radiative lifetime of the exciton and biexciton lines are of the same order as QW radiative lifetime, the large occupancies of the system ($i \geq 3$) significantly contribute to the QD emission, even at very low average number of excitons in the system. This results in the appearance of the XX sideband at low occupancy of the system. This behavior is in great contrast to what is observed with long radiative lifetime QDs such as self-assembled InAs QDs.

III. MODEL

We now give a quantitative description of the biexciton sideband by developing a simple model accounting for our

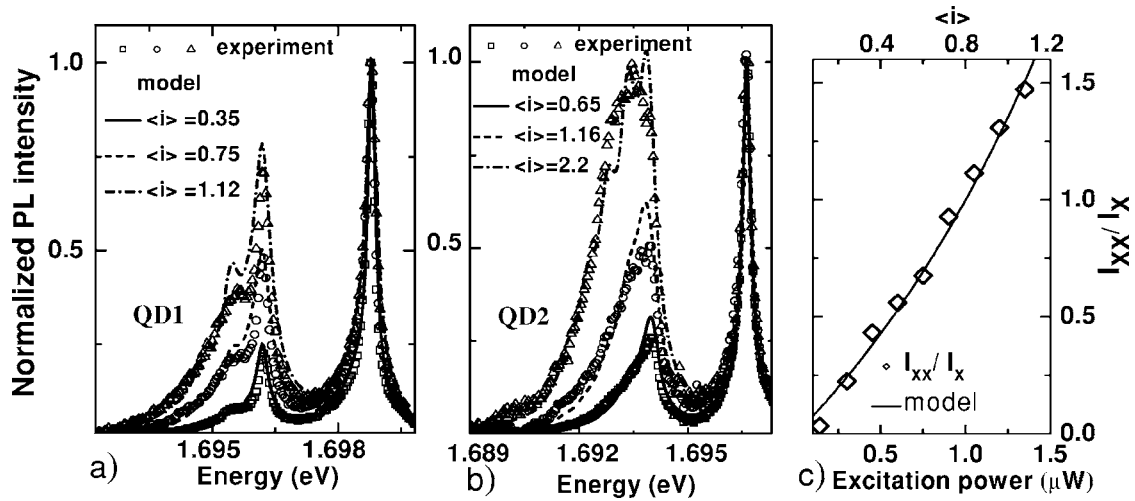


FIG. 3. Right: I_{XX}/I_X ratio as a function of excitation power for QD1. Symbols: experiment. Full line: fit. Top scale: average number of excitons $\langle i \rangle$ in the system. Left: symbols: experimental PL spectra measured for various $\langle i \rangle$ for QD1 (top) and QD2 (bottom). Full lines: calculated spectra.

experimental observations. In the following, we assume that the capture toward the ground state of the QD is instantaneous. This assumption is strongly supported by the very short risetime (≈ 30 ps) observed in time resolved measurements.¹² As a result, we consider that whenever the system contains $i \geq 2$ electron-hole pairs, two electron-hole pairs are in the QD ground state, $i-2$ are in the QW continuum state. We define p_i as the probability that the system contains i electron-hole pairs. Each probability p_i decays due to radiative recombination of the excitons inside the QD or the QW, with a decay time noted t_i . We have $t_1 = t_X$, $t_2 = t_{XX}$, and $1/t_i = 1/t_{XX} + (i-2)/t_{QW}$ for $i \geq 2$. The system occupation $i=1$ (resp. $i=2$) gives rise to an emission at the energy of the exciton $E_1 = E_X$ (resp. biexciton $E_2 = E_{XX}$) with a weight p_1/t_1 (resp. p_2/t_2). When $i \geq 3$, recombination in the QD ground state gives rise to an emission with weight p_i/t_{XX} .¹⁶ This emission is redshifted as compared to the unperturbed biexciton energy E_{XX} . Such a redshift of a QD emission line in presence of excitons in higher energy states has been theoretically analyzed in InAs QDs.¹⁷ It has been shown that the influence of the Coulomb interaction on the emission energy can be understood as follows: whenever the high energy state interacting with the biexciton state inside the QD is partially occupied, the biexciton ground state energy is reduced by the sum of the electron-electron and hole-hole Coulomb exchange terms. As a result, we expect a redshift of the emission, which is supposed to be larger when the population of the quantum well electron-hole pairs is large. In the following, we neglect the exchange interaction between excitons in the QW so that Coulomb interaction gives rise to only one additional line for each $i \geq 3$. We assume that the redshift of each line is simply proportional to the number of excitons in the QW: $E_i = E_{XX} - (i-2)\Delta E$. Full calculation of the redshift in multiexciton complexes indicates that this simplification holds as long as the number of excitons inside the excited states is small.¹⁸ We only need to consider at most four excitons in the QW state ($i \leq 6$) to account for the observed XX spectral line shape. We take

$\Delta E = 0.7$ meV as the only fitting parameter for all calculations.

We note $1/t_a$ the optical injection rate of *one* electron-hole pair in the system. $1/t_a = P/A$, where P is the excitation power and A describes the optical injection efficiency in the sample. The probabilities p_i are governed by the following rate equations

$$\frac{dp_i}{dt} = \frac{p_{i+1}}{t_{i+1}} + \frac{p_{i-1}}{t_a} - p_i \left(\frac{1}{t_i} + \frac{1}{t_a} \right).$$

The first two terms contribute to the increase of the p_i probability: radiative recombination of an exciton in the $i+1$ case and optical injection of an exciton in the $i-1$ case. The last two terms contribute to a decrease of the p_i probability: radiative recombination of an exciton and optical injection of an exciton in the i case.

The stationary solution of this system is given by $p_i = (p_0 \prod_{j=1}^i t_j) / (t_a)^i$ for $i \geq 1$. p_0 is obtained by the probability normalization $\sum_{i=0}^{\infty} p_i = 1$. t_X , t_{XX} , and t_{QW} have been measured for each QD in time resolved measurements so that we know every t_i .¹² We can then numerically calculate every p_i as a function of $t_a = P/A$. To determine A , we consider the intensity ratio $I_{XX}/I_X = (p_1/t_X) / (\sum_{j=2}^{\infty} p_j/t_{XX})$ which depends only on the parameter A through the p_i . By fitting this ratio as a function of P as shown in Fig. 3(c), we determine the value of A for all measurements. Then, each excitation power corresponds to an average number of excitons in the system, given by $\langle i \rangle = \sum_{j=0}^{\infty} j p_j$, as shown on the top scale of Fig. 3(c).

Finally, to calculate the emission spectra, we sum the contribution to the emission of each case i , with weight $q_1 = p_1/t_X$ at energy E_X for $i=1$ and $q_i = p_i/t_{XX}$ at E_i for $i \geq 2$ (see the lower part of Fig. 2). Each contribution is broadened by the same spectral function with unity area. This spectral function is taken as the sum of two Lorentzian functions so as to account for both the zero phonon line and the phonon sidebands of the exciton line.¹⁵

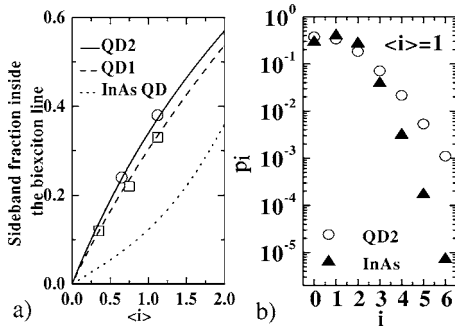


FIG. 4. (a) Symbol: Experimental sideband fraction inside the biexciton line for QD1 (square) and QD2 (circle). Lines: Calculated sideband fraction inside the biexciton line as a function of the average number of excitons in the system $\langle i \rangle$ for QD1, QD2 and a typical InAs QD. (b) p_i (log scale) as a function of i for $\langle i \rangle = 1$ for QD2 (circle) and a typical InAs QD (triangle).

Figure 3(a) presents both calculated and experimental spectra for QD1 for three excitation powers corresponding to three values of $\langle i \rangle$. Our model very well accounts for the spectral line shape of the biexciton line for various excitation powers. It also shows that the contribution of the biexciton sideband to the biexciton line is significant even for an average number of excitons in the system as low as 0.35. In Fig. 3(b), we present both calculated and measured spectra for another QD (QD2), which presents shorter radiative lifetimes ($t_X = 100$ ps and $t_{XX} = 60$ ps). For an average number of excitons around 2, the emission at the unperturbed biexciton energy is even smaller than the contribution of the sideband.

IV. DISCUSSION

We now compare the contribution of the sideband to the emission line for QD1 and QD2. The experimental sideband fraction in the biexciton line is reported in Fig. 4(a). For both $\langle i \rangle = 1.1$ and $\langle i \rangle = 0.7$, the fraction of the sideband in the biexciton line is larger for QD2 than QD1. We experimentally observe an influence of the QD radiative lifetime on the sideband fraction in the biexciton line. This trend is quantitatively accounted for by our model. In Fig. 4(a), we have plotted the calculated fraction of the biexciton signal emitted in the sideband for QD1 and QD2. This fraction is given by $I_{\text{sideband}}/I_{XX} = \sum_{j=3}^{\infty} p_j / \sum_{j=2}^{\infty} p_j$. We see that the calculated fraction is larger for QD2 than for QD1, as experimentally observed.

To complete this analysis, we analyze what is expected for InAs QDs which present much longer typical radiative lifetime (around 1–3 ns). First, let us analyze the PL spectra observed for a single InAs QD as a function of excitation power in Ref. 19. For low excitation power, only the exciton and biexciton line are observed. The first red shifted biexciton line (contribution $i=3$ of our sideband) is observed for high excitation power, only when the first excited state of the QD is filled. In this regime, no exciton is observed, and the emission is maximum in the excited state. High QD filling factors radiate mainly through the QD high energy states, in contrast to fast emitting monolayer fluctuation QDs. To be

more quantitative, we calculate the sideband contribution to the XX line for a typical InAs QDs. In our model, we have considered QDs with only one confined states. This analysis still holds for QD with excited states; we then consider a “mean excited state” with “an average radiative lifetime,” gathering all excited states of the QD and QW. We take an InAs QD exciton radiative lifetime around 1.5 ns, $t_{XX} = t_X/2$ and a typical two-dimensional lifetime for the high energy state $t_{QW} = 200$ ps.²⁰ In Fig. 4(a), we see that to observe a sideband fraction around 20%, an average number of 1.5 excitons in the system is needed in InAs QDs whereas an average number of only 0.5 is needed in GaAs QDs.

Finally, note that the radiative lifetime influences the sideband signal weight $q_i = p_i/t_{XX}$ through both $1/t_{XX}$ and p_i . Indeed, the stationary solution for the p_i depends on all the radiative lifetimes t_i . This effect is illustrated in Fig. 4(b), where p_i is plotted as a function of i for QD2 and a typical InAs QD for an average number of excitons in the system of $\langle i \rangle = 1$. p_i for $i \geq 3$ decreases much more rapidly with i for long radiative lifetime QDs than for fast emitting QDs. As a result, the XX sideband is much smaller for long radiative lifetime QDs than for short radiative lifetime QDs.

Studying carefully many measurements reported in various QDs systems as a function of excitation power, one finds that the appearance of the multiexciton lines is clearly correlated to the radiative time of QD ground states. In the pioneer work on GaAs monolayer fluctuation QDs,² low energy “satellite” can be seen on the low energy side of the biexciton line at low excitation power. Recently, Santori and co-workers have reported time resolved measurement in relatively fast emitting InGaAs self-assembled QDs, ($t_X = 479$ ps, $t_{XX} = 316$ ps).¹⁰ In their measurements, such a sideband also clearly appears in the low energy side of the biexciton line. On the contrary, on InAs QDs with very long radiative lifetime, multiexciton lines only appear for very high excitation density ($\langle i \rangle \approx 2-13$) when the system mainly radiates in its high energy states.^{17,19}

V. CONCLUSION

In conclusion, we have evidenced a strong influence of Coulomb interaction in the biexciton emission line of fast emitting single GaAs QDs. For a very small number of excitons in the system, it appears as a broad low energy sideband to the biexciton line, due to exchange interaction between the biexciton in the QD ground state and excitons in higher energy states. The appearance of this sideband at very low exciton density is the signature of fast emitting QDs. Our model gives an overall understanding of why the spectral feature on the biexciton is visible in some QDs and not in others. In the perspective of using single QDs to generate qubits, fast emitting QDs are needed. Our work shows that when the radiative decay of the QDs is fast, its Coulomb environment plays a crucial role in its emission, even at very low density.

ACKNOWLEDGMENTS

This work was partly supported by the “Région Ile de France” and the “Conseil Général de l’Essonne.”

*Electronic address: pascalle.senellart@lpn.cnrs.fr

- ¹For a review, see *Single Quantum Dots, Topics of Applied Physics* edited by P. Michler Springer Verlag, Heildeberg, (2003).
- ²K. Brunner, G. Abstreiter, G. Bohm, G. Trankle, and G. Weimann, *Phys. Rev. Lett.* **73**, 1138 (1994).
- ³J.-Y. Marzin, J.-M. Gérard, A. Izrael, D. Barrier, and G. Bastard, *Phys. Rev. Lett.* **73**, 716 (1994).
- ⁴E. Moreau, I. Robert, L. Manin, V. Thierry-Mieg, J. M. Gérard, and I. Abram, *Phys. Rev. Lett.* **87**, 183601 (2001).
- ⁵Filippo Troiani, Ulrich Hohenester, and Elisa Molinari, *Phys. Rev. B* **62**, R2263 (2000).
- ⁶X. Li, Y. Wu, D. Steel, D. Gammon, T. H. Stievater, D. S. Katzer, D. Park, C. Piermarocchi, and L. J. Sham, *Science* **301**, 809 (2003).
- ⁷D. Fattal, E. Diamanti, K. Inoue, and Y. Yamamoto, *Phys. Rev. Lett.* **92**, 037904 (2004).
- ⁸Matthew Pelton, Charles Santori, Jelena Vuckovic, Bingyang Zhang, Glenn S. Solomon, Jocelyn Plant, and Yoshihisa Yamamoto, *Phys. Rev. Lett.* **89**, 233602 (2002).
- ⁹J. Hours, S. Varoutsis, M. Gallart, J. Bloch, I. Robert-Philip, A. Cavanna, I. Abram, F. Laruelle, and J. M. Gérard, *Appl. Phys. Lett.* **82**, 2206 (2003).
- ¹⁰Charles Santori, Glenn S. Solomon, Matthew Pelton, and Yoshihisa Yamamoto, *Phys. Rev. B* **65**, 073310 (2002).
- ¹¹G. Bacher, R. Weigand, J. Seufert, V. D. Kulakovskii, N. A. Gippius, A. Forchel, K. Leonardi, and D. Hommel, *Phys. Rev. Lett.* **83**, 4417 (1999).
- ¹²J. Hours, P. Senellart, E. Peter, A. Cavanna, and J. Bloch, *Phys. Rev. B* **71**, 161306(R) (2005).
- ¹³A. Kiraz, S. Falth, C. Becher, B. Gayral, W. V. Schoenfeld, P. M. Petroff, Lidong Zhang, E. Hu, and A. Imamoglu, *Phys. Rev. B* **65**, 161303(R) (2002).
- ¹⁴E. S. Moskalenko, K. F. Karlsson, P. O. Holtz, B. Monemar, W. V. Schoenfeld, J. M. Garcia, and P. M. Petroff, *Phys. Rev. B* **66**, 195332 (2002).
- ¹⁵E. Peter, J. Hours, P. Senellart, A. Vasanelli, A. Cavanna, J. Bloch, J. M. Gérard, *Phys. Rev. B* **69**, 041307(R) (2004).
- ¹⁶We assume that the radiative lifetime of the biexciton is not changed by the presence of excitons in the QW.
- ¹⁷E. Dekel, D. Regelman, D. Gershoni, E. Ehrenfreund, W. V. Schoenfeld, and P. M. Petroff, *Phys. Rev. B* **62**, 11038 (2000).
- ¹⁸E. Dekel, D. Gershoni, E. Ehrenfreund, D. Spektor, J. M. Garcia, and P. M. Petroff, *Phys. Rev. Lett.* **80**, 4991 (1998).
- ¹⁹M. Bayer, O. Stern, P. Hawrylak, S. Fafard, and A. Forchel, *Nature (London)* **405**, 923 (2000).
- ²⁰Haiping Yu, Sam Lycett, Christine Roberts, and Ray Murray, *Appl. Phys. Lett.* **69**, 4087 (1996).